Dielectric Enrichment of 1-(9-Anthryl)-3-(4-*N*,*N*-dimethylaniline) Propane in Hexane−Ethanol Mixtures

Mazdak Khajehpour and John F. Kauffman*

Department of Chemistry, University of Missouri-Columbia, Columbia, Missouri 65211-7600

Received: April 17, 2000

1-(9-Anthryl)-3-(4-*N*,*N*-dimethylaniline) propane (ADMA) is known to form an emissive "sandwich heteroexcimer" (SH) in the excited state. The SH state has a distinct emission spectrum that can be characterized as a single Gaussian peak. We have studied preferential solvation of the ADMA SH state in binary hexane−ethanol mixtures by monitoring its peak emission energy. The results are analyzed with a theory of preferential solvation by dielectric enrichment (Suppan, P. *J. Chem. Soc., Faraday Trans.* **1987**, *83*, 495). Our analysis demonstrates a significant influence of mixture dielectric nonideality on solvatochromism, and this effect can be misinterpreted as specific solvent−solute interaction if it is not treated properly. We are able to separate the influence of mixture nonideality from the influence of dielectric enrichment, and conclude that specific interactions do not contribute to the observed solvatochromic shift in the ADMA−hexane−ethanol system. The analysis also indicates that solvent−solute interactions in this system can be adequately described with a continuum model. We calculate the composition of the ADMA solvation shell and find that it is enriched in ethanol by ∼50% over the bulk composition. ADMA is identified as an excellent probe of dielectric enrichment in complex environments.

I. Introduction

When a polar solute is dissolved in a binary solvent mixture, it interacts differently with each of the solvent components. It is therefore reasonable to expect that the composition in the near vicinity of the solute will be different from the bulk composition. This concept of preferential solvation has long been used qualitatively to rationalize measured solute properties that deviate from a linear dependence on solvent composition.[1] Preferential solvation can occur either through specific interactions of the solute with one of the solvent components or through dielectric enrichment. Specific interactions occur with solvent molecules that are so close to the solute that intermolecular bonds, such as hydrogen bonds, can form. These interactions are usually directional and reflect a strong interaction between the solute and a single solvent molecule. On the other hand, dielectric enrichment derives from an increased concentration of the polar solvent component throughout the solvation sphere due to its attraction to the solute charge distribution. Enrichment of the solvation sphere has spherical symmetry to a good approximation, and can be analyzed under the assumption of a continuum solvent shell model.[2] Although these two mechanisms are different, they often occur in tandem because functional groups that participate in specific interactions often have very large dipole moments.[3]

Preferential solvation is often correlated with spectral measurements using the expression[4−11]

$$\delta_{AB} = y_A\delta_A + y_B\delta_B \qquad (1)$$

in which δ_A and δ_B are spectral properties (peak positions, peak intensities, kinetic rate constants, etc.) of the solute measured in neat solvents A and B, and δ_{AB} is the same property measured in a binary mixture of the solvents A and B. Equation 1 relates δ_{AB} to δ_A and δ_B using the parameters y_A and $y_B = 1 - y_A$, where y_A and y_B are considered to be local compositions of the solvent components near the solute. Although eq 1 serves as an operational definition of preferential solvation, it does not necessarily provide an accurate measure of the local composition because there is no theoretical justification to the assumption that δ_{AB} is a mole fraction weighed average of δ_A and δ_B. Ben-Naim points out that in general, eq 1 will result in different values of y_A for different spectroscopic measurements on the same chemical system.[11,12] Thus a more rigorous theoretical approach is required to obtain the local solvent composition in the near vicinity of the solute molecule.

A viable alternative to eq 1 is the theory of dielectric enrichment as proposed by Suppan.[2] This theory explains preferential solvation in terms of a dielectric continuum model and has been applied to several binary solvent systems.[2,3,13−17] When a dipole is immersed in a mixed solvent system, its immediate environment is perturbed by differential attraction toward the more polar solvent component, resulting in diffusion of the more polar component toward the dipole. Ultimately, equilibrium is obtained when the favorable interaction between the dipole and the polar component is balanced against the loss in entropy due to the demixing that occurs in the vicinity of the solute. The thermodynamic expression thus obtained provides an unambiguous means of characterizing the local solvent composition. It can also provide insight as to whether the origin of preferential solvation is an interaction between the solute and the solvent reaction field, or a specific interaction such as hydrogen bonding.[2,3,13−15]

In this work, we measure fluorescence spectra of ADMA (1-[9-anthryl]-3-[4-*N*,*N*-dimethylaniline] propane, see Figure 1) in neat solvents and in *n*-hexane−ethanol mixtures. ADMA is nonpolar in the ground state, but forms an emissive, excited-state intramolecular charge-transfer complex following photoexcitation of the anthracene moiety. The position of the exciplex

10.1021/jp0014519 CCC: $19.00
Published on Web 07/11/2000

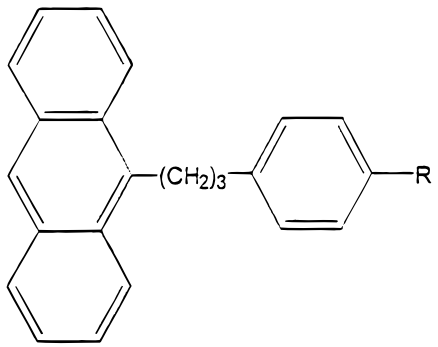

Figure 1. Structure of ADMA (R = $N(CH_3)_2$) and APP (R = H). See Figure 3 for representative structures.

emission peak depends on solvent polarity. We first demonstrate that the exciplex peak energy is linear in the Lippert−Mataga solvent polarity function[18] in neat solvents, but not in *n*-hexane−ethanol mixtures. The mixture results are then analyzed according to the theory of dielectric enrichment to determine the local composition, demonstrating that dielectric enrichment is the mechanism of preferential solvation in the system.

II. Experimental Section

ADMA and APP (1-(9-anthryl)-3-(phenyl) propane, Figure 1) were synthesized according to methods outlined previously.[19] All solvents were obtained in the purest form available from Aldrich. They were degassed by bubbling argon and used without further purification. All sample concentrations were 10^{-5} M.

The fluorescence spectra of the solutions where collected in a home-built scanning T-format fluorimeter. The emission was collected with a photomultiplier tube through one arm, and the fluorescence at a fixed wavelength was collected synchronously and simultaneously through the other arm to correct for fluctuations in the emission intensity due to sample and instrumental conditions. The emission slit widths were set at 1.5 nm, giving 3-nm resolution. Samples were thermostated at 25 °C, unless noted otherwise. Dielectric constants of solvent mixtures were obtained from capacitance measurements using a thermostated capacitance cell and a capacitance instrument of our own design.[20]

III. ADMA Charge Transfer State Formation: Dynamics and Spectroscopy

Figure 2a demonstrates two distinct contributions to the fluorescence spectrum of ADMA dissolved in tetrahydrofuran after excitation of the anthracene moiety at 387 nm. The emission at wavelengths <450 nm resembles the anthracene spectrum. These emissions are observed in both ADMA and APP spectra and have been assigned to emission from the locally excited anthracene.[21] The broad emission in the 450−600-nm range is only observed in the ADMA spectrum and has been assigned to emission from a folded charge-transfer exciplex.[22] These spectral features mimic those of the bimolecular anthracene−dimethylaniline complex.[23] Fluorescence lifetime studies of both features have elucidated the mechanism for charge-tranfer formation illustrated in Figure 3.[21,22,24−28] Three important solute configurations are identified in Figure 3 as the locally excited (LE) configuration, the loose heteroexcimer (LH) configuration, and the sandwich heterexcimer (SH) configuration. The LE configuration is an extended conformation representative of the solute conformation in the ground state. The SH configuration represents the conformation of an emissive charge-transfer excited state. This state is the low energy excited-state conformation in nonpolar solvents and in solvents of modest polarity ($\epsilon = 5-20$). In nonpolar solvents the LE state must attain the folded conformation before charge transfer occurs. The rate of charge-transfer state formation is limited by conformational diffusion, and exhibits a power law dependence on solvent viscosity.[19,24] The SH configuration has the lowest energy in solvents of modest polarity, but an extended charge-transfer configuration (the LH state) is the low energy form in highly polar solvents.[25,28] As a result, the charge-transfer band shown in Figure 2a is extremely weak in highly polar solvents such as acetonitrile.[25] (The LH state has a very low fluorescence quantum yield, though it can be observed by transient absobance.[25,27]) In solvents of modest polarity, the LH can form directly from the LE state, and subsequently Coulombic attraction between the charge-separated moieties results in accelerated formation of the charge-transfer state.[25,27] Competition between the diffusive and accelerated pathways is mediated by solvent polarity through its influence on the energy of the LH intermediate, as illustrated in Figure 3.

The spectrum of ADMA is influenced by solvent polarity in two ways. First, the intensity of the charge-transfer band depends on the rate of SH formation and on the energetics of the LH intermediate, as already discussed. Second, the peak position of the charge transfer band is governed by solvent stabilization following the formation of the charge transfer band. The absorbance spectrum of ADMA undergoes a very small shift (~2 nm) when the solvent is changed from *n*-hexane to ethanol, indicating that the dipole moment of ADMA in the ground state is small. On the other hand the excited state dipole moment is large after formation of the charge-transfer state, and the energy of this configuration is expected to depend strongly on solvent polarity. The resulting solvatochromic shift is dynamic because the solute dipole is created instantaneously when the charge transfer occurs. In neat solvents we expect the dynamics to be governed by solvent rotational motion, with a time scale that is short compared with the rate of charge transfer state formation.[29−32] In solvent mixtures, on the other hand, the dynamics of solute stabilization is governed by diffusion of the polar solvent component into the solvation sphere of the SH configuration of ADMA, and is expected to occur on a nanosecond time scale.[2,17] This fact complicates interpretation of time-resolved emission from ADMA. However, the SH state is extremely long-lived (>100 ns in the absence of molecular oxygen). [19,25−27] Thus, the time-integrated charge-transfer emission peak energy is representative of the equilibrium stabilization experienced by the solute and is therefore an excellent probe of dielectric enrichment.[2]

We characterize the peak position as follows. Spectra of APP and ADMA are collected under identical conditions. The APP spectrum is subtracted from the ADMA spectrum, and the resulting difference spectrum is representative of emission from the charge-transfer complex.[19,24] We model the resulting charge-transfer band as a Gaussian peak using nonlinear regression (SigmaPlot), as shown in Figure 2b. Peak positions thus obtained are given in Table 1, and the uncertainties are dominated by the 3-nm resolution of the fluorimeter. Peak energies of the ADMA charge-transfer band measured in neat solvents are plotted in Figure 4a against the solvent dependent term in the Lippert−Mataga peak energy equation[18]

$$J = -\frac{\mu^2}{a^3}\cdot\frac{1}{4\pi\epsilon_0}\left[\frac{2(\epsilon-1)}{2\epsilon+1} - \frac{n^2-1}{2n^2+1}\right] + J_0 \qquad (2)$$

Hereafter we refer to this type of plot as a Lippert−Mataga

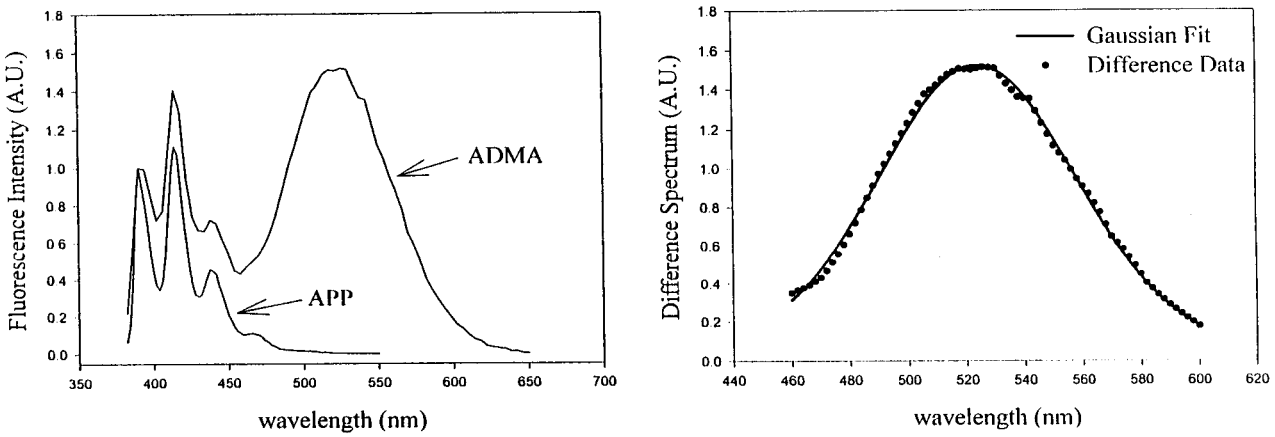

Figure 2. (a) Fluorescence spectra of ADMA and APP in tetrahydrofuran (THF), illustrating their similarity in the 400−480 nm region. (b) Difference spectrum after subtraction of the APP spectrum from the ADMA spectrum. The circles are difference data points, and the line is a regression fit to a Gaussian peak shape. Center frequencies are taken from the results of the regression.

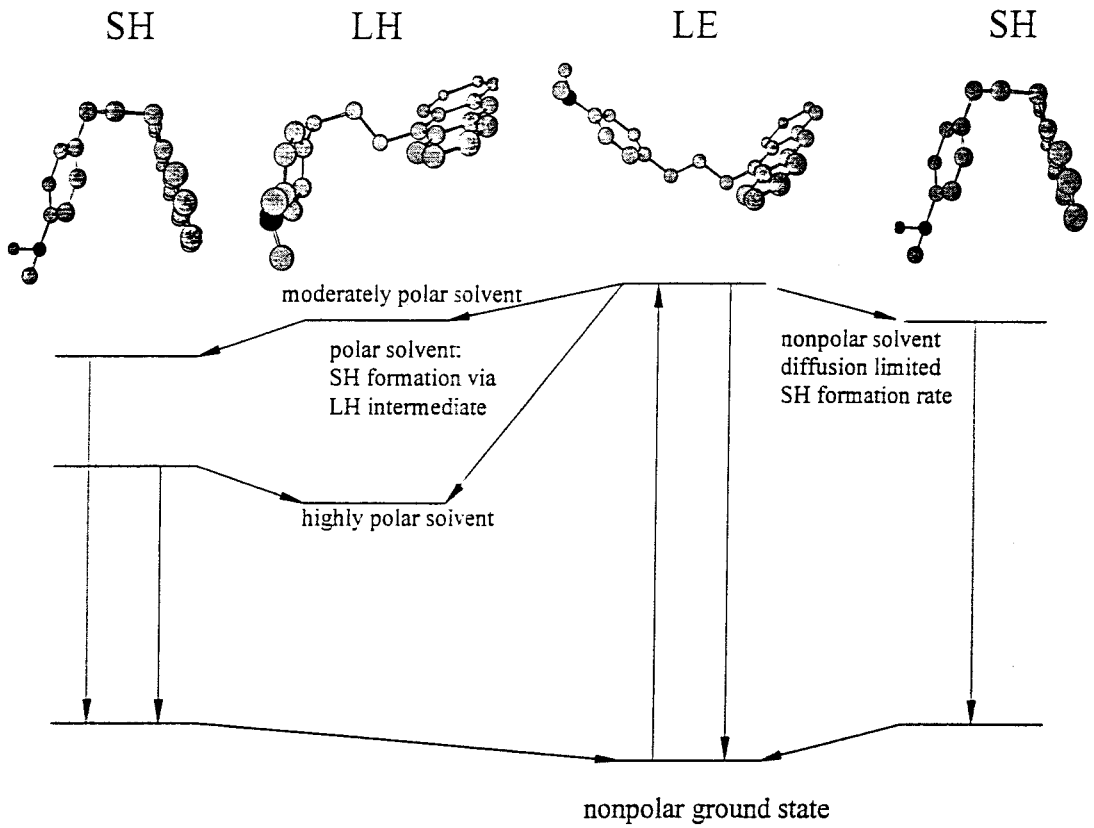

Figure 3. Energy level scheme that governs excited state isomerization kinetics of ADMA. The scheme demonstrates that sandwich heteroexcimer (SH) state formation is mediated by both solvent viscosity and solvent polarity. In polar solvents, the favored pathway to the SH state is through the charge-separated loose heteroexcimer (LH) intermediate. The weakly emissive LH state becomes the low-energy configuration in highly polar solvents. Solvent relaxation occurs after formation of the charge-transfer state of the molecule.

(LM) plot and to the bracketed term as the LM polarity function. In eq 2, J is the peak energy, and J_0 is the vacuum energy, and ϵ and n are the solvent dielectric constant and refractive index, respectively. The plot is linear, consistent with previous reports.[21] The slope of the plot (51.1 kJ/mol) is $\mu^2/(2a^3)$ and the measured dipole moment is 11.7 D (39.9×10^{-30} C·m), obtained from electrooptical emission measurements.[33] This value gives $a = 4.45$ Å, which is within 3% of the van der Waals radius (~4.32 Å) obtained using the method of Bondi,[34] assuming that the solute is spherical. The intercept of this plot predicts a peak energy in a vacuum of 457 nm, which is in excellent agreement with the peak position measured in supersonic jet spectra of ADMA when sufficient internal energy is provided for the isomerization reaction.[19b] Peak energies measured in *n*-hexane−ethanol mixtures are also given in Table 1. Comparison of these results with the neat liquid regression line is shown in Figure 4b, which demonstrates a marked deviation from linearity. In Section VI we analyze the mixed liquid results using the theory developed by Suppan and co-workers, and demonstrate that the deviation from linearity results from dielectric enrichment of the solvation sphere.

IV. Ideal Mixture, Single-Shell Theory of Dielectric Enrichment

The following is a concise summary of the theory of dielectric enrichment as developed by Suppan and co-workers.[2,3,14,35,36]

TABLE 1: Peak Positions of the ADMA Sandwich Heteroexcimer (SH) Emission Peak in Pure Solvents and in *n*-Hexane−Ethanol Mixtures[a]

solvent	SH peak (nm)	fitting error (nm)	peak energy (kJ/mol)
n-hexane (1)	474.6	0.4	252
cyclohexane (2)	473.2	0.5	253
dibutylether (3)	492.3	0.1	243
diethylether (4)	504.2	0.2	237
t-amylalcohol (5)	514.6	0.6	232
n-butylchloride (7)	509.00	0.03	235
ethylacetate (6)	522.6	0.2	229
tetrahydrofuran (8)	523.9	0.1	228
methylenechloride (9)	526.1	0.2	227
isoamylalcohol (10)	522.9	0.2	229
ethanol (11)	537.1	0.3	223
10% ethanol−*n*-hexane	492.2	0.4	243
19.8% ethanol−*n*-hexane	502.0	0.2	238
28.7% ethanol−*n*-hexane	513.0	0.6	233
40.9% ethanol−*n*-hexane	516.8	0.2	231
50.2% ethanol−*n*-hexane	520.5	0.2	230
60.8% ethanol−*n*-hexane	523.7	0.1	229
80.1% ethanol−*n*-hexane	528.7	0.2	226

[a] The numbers beside pure solvents match the number labels in Figure 4a. Peak energies are given in nm and in kJ/mol. The error listed in the table is the standard error of the peak position from the nonlinear regression analysis. In all cases, this error is small compared with the monochromator slitwidth of 1.5 nm and the spectral resolution of 3 nm. Error bars in plots are based on the resolution uncertainty, which corresponds to an uncertainty of ±1.5 kJ/mol.

The molecule in solution is approximated in the Onsager model[37] as a point dipole of magnitude μ located at the center of a spherical cavity of radius a, immersed in a continuous dielectric medium. Suppan[35] defines the stabilization energy ΔU relative to the vacuum as

$$\Delta U = -\frac{\mu^2}{2a^3}F = -\frac{\mu^2}{2a^3}\left[\frac{1}{4\pi\epsilon_0}\cdot\left(\frac{2(\epsilon-1)}{2\epsilon+1}\right)\right] \tag{3}$$

where F is the Onsager solvent polarity function, ϵ is the solvent dielectric constant, and ϵ_0 is the permittivity of free space. If the electronic spectrum of the molecule is taken in two different solvents, the difference in the peak energies of the molecule in the two solvents is $\Delta(\Delta U) = (-\mu^2/a^3)\Delta F$, where ΔF is the difference between the F values of the two solvents.[35] It is interesting to note that Suppan uses an expression for the peak energy that does not include the polarizability of the solvent, which is the second term of the LM solvent polarity function. However, this term is effectively constant for all solvents depicted in Figure 4 (0.19 ± 0.01), and therefore has no effect on ΔF, the solvent dependent factor in Suppan's theory. This fact is an essential element of the analysis presented in Section V.

Qualitatively preferential solvation occurs when the composition of the binary solvent in the near vicinity of the solute differs considerably from the bulk value. Thermodynamically preferential solvation is the result of two competing phenomena; stabilization of the dipole, which prefers to be solvated by the polar component of the solvent mixture, and entropy, which opposes any local variation from the bulk composition. This competition can be quantitatively defined from the free energy expression,

$$\Delta A = \Delta E - T\Delta S \tag{4}$$

Consider the effect of a dipole μ on a binary solvent mixture of bulk composition x_p and x_n, where x_p and x_n are the polar and nonpolar mole fractions, respectively. Figure 5 depicts a model of the local solvent environment in which a solvent shell of thickness Δr located at a distance r from the cavity center interacts with the point dipole ($\Delta r = 2b$, where b is the van der Waals radius of the solvent). For the first solvation shell, $r = a + b$. A finite dipole causes demixing of the solvent in the vicinity of the solute, especially in the first solvation shell. The equilibrium composition of the shell is obtained by minimizing the free energy expression against the Onsager solvent polarity function,

$$\frac{d(\Delta E)}{dF} - T\frac{d(\Delta S)}{dF} = 0 \tag{5}$$

The entropy of mixing is given by

$$\Delta S = y_n R \ln\left(\frac{x_n}{y_n}\right) + y_p R \ln\left(\frac{x_p}{y_p}\right) \tag{6}$$

where R is the ideal gas constant and y_n and y_p are the mole fractions of the nonpolar (n) and polar (p) solvent components in the local (y) vicinity of the solvent. The binary solvent is considered to be an ideal dielectric if the following relations hold:

$$F_{i,bulk} = x_n F_n + x_p F_p \tag{7a}$$

$$F_{i,local} = y_n F_n + y_p F_p \tag{7b}$$

where F_p and F_n are the solvent polarity functions of the pure polar and nonpolar components of the solvent, respectively, and $F_{i,bulk}$ and $F_{i,local}$ are the ideal mixture polarity functions of the solvent in the bulk and in the near vicinity of the solute, respectively. The entropic term is evaluated with the aid of eq 8:

$$\frac{d(\Delta S)}{dy_p} = R \ln\left(\frac{x_n y_p}{x_p y_n}\right) \tag{8}$$

Applying a chain rule for the derivative in eq 5, the shell contribution to the entropic term is obtained as follows:

$$\frac{d(\Delta S)}{dF} = \frac{4\pi R r^2 \delta \Delta r}{M\Delta F_{p-n}} \ln\left(\frac{x_n y_p}{x_p y_n}\right) \tag{9}$$

where $\Delta F_{p-n} = F_p - F_n$, and M and δ are, respectively, the mean molecular weight and density of the two solvent components. The solvent shell with an Onsager polarity function F, contributes to the stabilization of the dipole via eqs 10 and 11:

$$\Delta E = \Delta U(r) - \Delta U(r+\Delta r) = \frac{-3}{2}\mu^2 r^{-4}\Delta r F \tag{10}$$

$$\frac{d(\Delta E)}{dF} = \frac{-3}{2}\mu^2 r^{-4}\Delta r \tag{11}$$

Equations 9 and 11 lead to the following expression for the local composition at r:

$$\frac{y_n}{y_p} = \frac{x_n}{x_p}\exp(-Z_{ps}) \tag{12}$$

where Z_{ps} is the index of preferential solvation and characterizes the local solvent composition (as discussed later):

$$Z_{ps} = \frac{C\mu^2 M\Delta F_{p-n}}{TR\delta r^6} \tag{13}$$

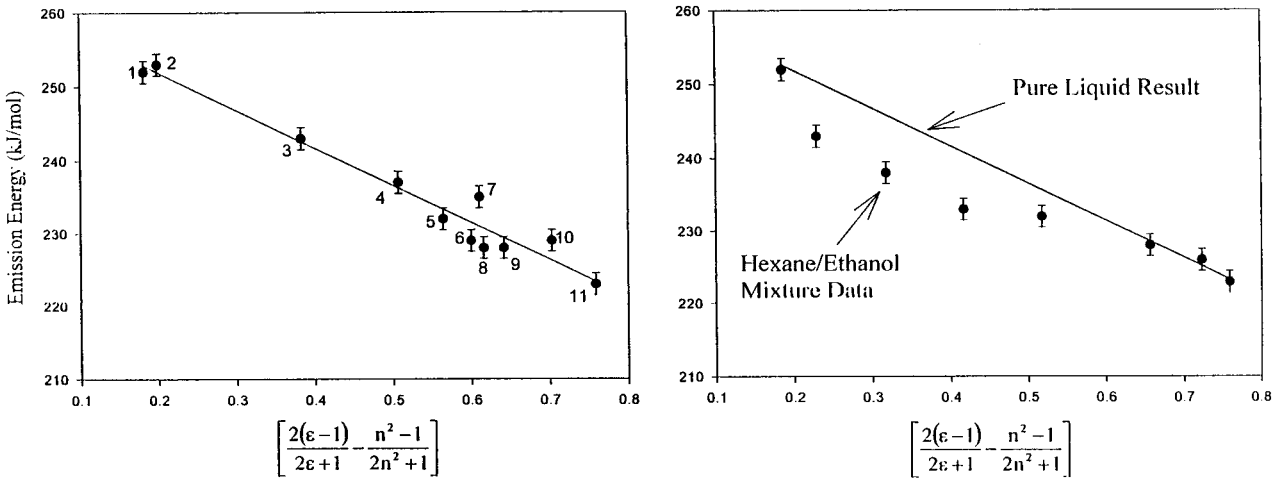

Figure 4. (a) LM plot of the ADMA sandwich heteroexcimer (SH) emission in pure solvents. Numbers in the plot match the solvents given in Table 1. The linear relationship indicates that solvent−solute interactions do not significantly distort the solute charge distribution in the SH configuration. (b) LM plot of the SH emission in *n*-hexane−ethanol mixtures. Deviation from linearity indicates preferential solvation of the SH state by ethanol.

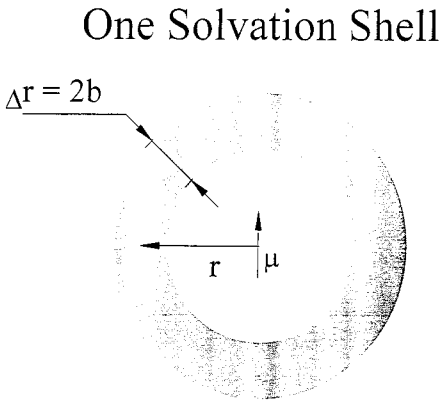

Figure 5. Model of the local solvent environment. Parameters illustrate the quantities of interest in Suppan's model: r is the distance from the center of the spherical cavity to the center of the solvation shell of interest; $\Delta r = 2b$ is the width of the solvation shell of interest, and is twice the radius, b, of the solvent molecules; and the first solvation shell has $r = a + b$.

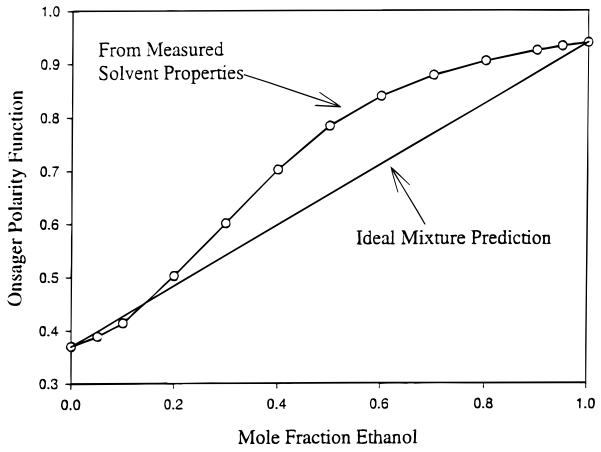

Figure 6. Solvent polarity function calculated from measured values of permittivity (ϵ) and refractive index (n) for *n*-hexane−ethanol mixtures versus ethanol mole fraction. The line represents the prediction for an ideal dielectric mixture with pure solvent properties identical to hexane and ethanol.

The constant C is a numerical constant formally equal to $3/(8\pi)$ when both the solvent and solute are spherical. The constant C is sometimes considered to be an empirical parameter of the system that depends on the shape of the solvent and solute molecules.[2,13] In our analysis, we use $C = 3/(8\pi)$.

Equations 12 and 13 are analytical results obtained for a single solvent shell around the solute. To find the total stabilization energy, an integration over all solvent shells is required. The integration does not yield an analytical result. Suppan and coworkers[2,35,36] have examined the numerical integration in some detail, and have concluded that in general, >90% of the total solute−solvent interaction energy is accounted for by the first solvent shell.[2] In the remainder of this section, the single shell approximation is made, and the analytical solution for the stabilization energy due to the first solvation shell can be written as

$$\Delta U = -\frac{\mu^2}{2a^3}F_{\text{eff}} \cong -\frac{\mu^2}{2a^3}\left[F_{\text{n}} + \left(1 + \frac{x_{\text{n}}}{x_{\text{p}}}\exp(-Z_{\text{ps}})\right)^{-1}\Delta F_{\text{p-n}}\right] \quad (14)$$

Here ΔU is the equilibrium dipole stabilization energy and F_{eff} is the actual solvent polarity experienced by the dipole. The second equality reflects the value of F_{eff} in the single shell approximation for an ideal mixture. The parameter Z_{ps} can be evaluated from solvent and solute parameters (eq 13) by assuming that $r = a + b$ for the first solvation shell. If one knows μ, a, and b, then ΔU can be calculated directly and compared with measured peak energies. A detailed analysis of our data based on eq 14 will be made in Section VI.

V. Preferential Solvation in Nonideal Mixtures

Equation 14 is derived under the assumption that the solvent mixture is ideal (i.e., eqs 7a and 7b are correct). We have tested this assumption by direct measurement of solvent dielectric constants for *n*-hexane−ethanol mixtures. Ethanol is a hydrogen-bonding liquid and, intuitively, we expect that ethanol and hexane will form a nonideal dielectric system. The theory of significant structures[38] predicts that the compositional dependence of the dielectric constant of mixtures with hydrogen-bonding components can be expressed in terms of a third-order polynomial. Using our experimental values obtained from capacitance measurements, the dielectric constant of a *n*-hexane−ethanol mixture can be expressed as

$$\epsilon_M = 1.943 - 1.120x_p + 16.89x_p^2 + 6.607x_p^3 \quad (15)$$

Refractive indices for *n*-hexane−ethanol mixtures have been interpolated from the data of Orge et al.[39] These results have been used to calculate the Onsager and LM solvent polarity functions versus composition for *n*-hexane−ethanol mixtures, and the results are plotted in Figure 6. Clearly, hexane and ethanol do not form an ideal dielectric mixture. Note, however, that the peak energies in Figure 4b are plotted versus measured values of the solvent polarity function, and in the absence of preferential solvation the peak energy will still be linear in this function. Thus, the results of Figure 4b are an unambiguous reflection of preferential solvation around the ADMA molecule. On the other hand, the results in Figure 6 call into question the ideal mixture approximation, and therefore the validity of eq 14. Suppan addresses this issue in the following manner. A quantity referred to as the nonlinearity ratio, ρ, expresses the mean deviation of the measured Onsager Polarity Function from the linear prediction based on eq 7. ρ is defined in general as

$$\rho = \frac{2\int(F_{meas} - F_{i,bulk})dx_p}{\Delta F_{p-n}} \quad (16)$$

where F_{meas} is a measured value of the Onsager Polarity Function versus mixture composition, $F_{i,bulk}$ is the ideal, calculated quantity versus composition based on eq 7a, and ΔF_{p-n} is the difference between the value of the quantity in pure polar (p) and nonpolar (n) solvent components. The difference between the measured and ideal quantity is integrated over the entire range of possible compositions from 0 to 100% polar component. An ideal, linear response results in a nonlinearity ratio of zero, and any deviation from a value of zero reflects the nonlinearity of the measured quantity.

The parameter ρ can be decomposed into a sum of two contributions; $\rho_{ni,bulk}$ resulting from the nonideality of the mixture in the bulk, and ρ_{ps} resulting from preferential solvation in the local solvation sphere. Thus, the total mean deviation from linearity is given by

$$\rho_t = \rho_{ni,bulk} + \rho_{ps} \quad (17)$$

where ρ_t is reflected in the measured peak energy compared with the linear prediction based on bulk neat solvent properties. We calculate ρ_t from spectral energies as

$$\rho_t = \frac{2\int(J_{meas} - J_{i,bulk})dx_p}{(\Delta J_{p-n})} \quad (18)$$

where J_{meas} is the measured peak energy in the solvent mixture, and $J_{i,bulk}$ is the ideal mixture peak energy calculated from the LM plot, assuming eq 7a is valid. It differs formally from Suppan's expression, eq 16, in that it includes a polarizability term. In practice, however, the difference in the polarizability terms between hexane and ethanol in the integrand and in the denominator is extremely small, on the order of 0.5% of the permittivity term, and therefore is negligible. Thus for binary solvent systems in which the component refractive indices are nearly equal, the definition given by eq 18 collapses into eq 16. In rare instances where solvents of substantially different refractive indices are used, one must exercise care in the use of solvatochromic peak enegies to characterize solvent stabilization energies.

Similarly, the nonlinearity resulting from bulk solvent nonideality can be determined from the values of the solvent polarity function calculated from measured bulk solvent properties,

$$\rho_{ni} = \frac{2\int(F_{meas,bulk} - F_{i,bulk})dx_p}{\Delta F_{p-n}} \quad (19)$$

This integral reflects the area between the line and the curve in Figure 6. The difference between ρ_t and ρ_{ni} gives ρ_{ps}, which is the quantity of interest in this study.

The previous discussion indicates that ρ_{ps} is the nonlinearity ratio of the system after subtraction of the contribution from nonideality. Thus, we can now interpret ρ_{ps} within the ideal mixture approximation, beginning with the expression

$$\rho_{ps} = \frac{2\int(F_{i,local} - F_{i,bulk})dx_p}{\Delta F_{p-n}} \quad (20)$$

where eqs 7a and 7b are used for the quantities in the integral. With the aid of eq 12, the integrand can be written in terms of x_p and solved analytically to give

$$\rho_{ps} = \frac{1 + e^{-Z_{ps'}}}{1 - e^{-Z_{ps'}}} + \frac{-2Ze^{-Z_{ps'}}}{(1 - e^{-Z_{ps'}})^2} \quad (21)$$

where the prime on $Z_{ps'}$ indicates that the index of preferential solvation is calculated via the nonlinearity ratio method. Thus, ρ_{ps} can be extracted from measured values of ρ_t and ρ_{ni}, and $Z_{ps'}$ can be calculated from ρ_{ps} using eq 21. In principle, $Z_{ps'}$ is equivalent to Z_{ps} if the single shell approximation is correct.

VI. Analysis of Local Composition

Calculation of Z_{ps} is tantamount to finding the local composition of the solvent around the solute molecule through eq 12. The theory just described offers two independent methods for calculating Z_{ps}. This parameter can be calculated in the ideal mixture−single shell approximation directly from eq 13, and it can be calculated after correction for solvent nonideality using eqs 17−21. In addition, a direct method to determine an effective experimental Z value (Z_{exp}) can be developed by inversion of eq 14. The latter method gives a quantity that is conceptually similar to the value of ρ_t in the sense that it includes contributions from both preferential solvation and solvent mixture nonideality. We evaluate Z by these methods in this section and discuss the relationship between each measure of Z.

Calculation of Z_{ps} via eq 13 requires the estimation of several parameters, including solvent density, δ, solvent molar mass, M, and the distance between the cavity center and the center of the first solvation sphere, r. Suppan uses mean values for M and δ, which for the *n*-hexane−ethanol system are 66 g/mol and 0.723 g/cm^3, respectively. We have chosen to use the bulk-mole-fraction-weighted molar mass, and the mixture densities are interpolated from measurements.[40] Table 2 presents Z_{ps} values determined for three separate measures of r because r is the parameter whose value most strongly influences Z_{ps}. We suggest that the most objective measure of r is the bulk-mole-fraction-weighted van der Waals radius of the solvent components. Though this value does not reflect the influence of preferential solvation on the width of the solvation sphere, it provides the most realistic 0th order approximation to the correct shell width. We have also calculated Z_{ps} using the ethanol van der Waals radius and the hexane van der Waals radius because these two values must bracket the correct radius.[41] Table 2 indicates that Z_{ps} calculated using the bulk-mole-fraction-

TABLE 2: Calculation of *Z* by Equation 13 versus Bulk Mole Fraction of Ethanol[a]

EtOH, mol %	radius value	*b* (Å)	*M* (kg/mol)	δ (kg/m^3)	*Z*
10	EtOH radius	2.03	0.082	660	0.74
	hexane radius	2.58	0.082	660	0.45
	bmfw radius	2.52	0.082	660	0.47
19.8	EtOH radius	2.03	0.078	666	0.70
	hexane radius	2.58	0.078	666	0.43
	bmfw radius	2.47	0.078	666	0.47
28.7	EtOH radius	2.03	0.075	670	0.67
	hexane radius	2.58	0.075	670	0.41
	bmfw radius	2.42	0.075	670	0.47
40.1	EtOH radius	2.03	0.070	682	0.62
	hexane radius	2.58	0.070	682	0.37
	bmfw radius	2.36	0.070	682	0.45
50.2	EtOH radius	2.03	0.066	692	0.57
	hexane radius	2.58	0.066	692	0.35
	bmfw radius	2.30	0.066	692	0.45
60.8	EtOH radius	2.03	0.062	706	0.53
	hexane radius	2.58	0.062	706	0.32
	bmfw radius	2.24	0.062	706	0.43
80.1	EtOH radius	2.03	0.054	735	0.44
	hexane radius	2.58	0.054	735	0.27
	bmfw radius	2.13	0.054	735	0.41
	mean parameters	2.31	0.066	723	0.42

[a] The molar mass (*M*) is calculated as mole-fraction-weighted mass of the mixture, and densities (δ) are determined from measurments. In all cases, the cavity radius, *a*, is given the ADMA van der Waals radius of 4.32 Å. *Z* is calculated for three values of the solvent shell halfwidth, *b*: (1) *b* = ethanol (EtOH) van der Waals radius (2.03 Å); (2) *b* = *n*-hexane van der Waals radius (2.58 Å), and (3) *b* = bulk mole fraction weighted (bmfw) radius. *Z* was also calculated for mean (arithmetic average) parameter values.

weighted radius has an average value of 0.45, and only varies by ± 5% across the entire composition range. It is also nearly identical to Z_{ps} calculated from mean parameter values.

Note that eq 13 is based on the ideal mixture assumption, and the resulting Z_{ps} value only reflects the contribution of preferential solvation to the solute charge-transfer emission peak energy.

Comparison of Z_{ps} with the $Z_{ps'}$ determined via the nonlinearity ratio concept is instructive. Using eq 18, we obtain a nonlinearity ratio of $\rho_t = 0.383$ from our spectroscopic measurements. Application of eq 19 to the calculation of ρ_{ni} using measured values of bulk refractive indices and dielectric constants gives $\rho_{ni} = 0.22$. From these values and eq 17, $\rho_{ps} = 0.163$, and eq 21 can be solved to find $Z_{ps'} = 0.5$. From the nonlinearity ratio method, $Z_{ps'}$ is in excellent agreement with the value of Z_{ps} calculated in the ideal mixture−single shell approximation. Agreement between $Z_{ps'}$, which is derived from experimental data, and Z_{ps}, which assumes that dielectric enrichment is the sole contributor to the solvatochromic shift, confirms that dielectric enrichment is responsible for preferential solvation around the ADMA sandwich heteroexcimer. Note that in the absence of a thorough analysis, the influence of nonideality can be misinterpreted and lead one to conclude that specific interactions are at play.

Equation 14 can be written as the difference, $\Delta(\Delta U)$, between the hexane peak position and the mixture peak position. Inverting the resulting expression gives

$$\frac{1}{\Delta(\Delta U)} = -\frac{2a^3}{\mu^2 \Delta F_{p-n}}\left[1 + \frac{x_n e^{-Z_{exp}}}{x_p}\right] \qquad (22)$$

We have substituted Z_{exp} for Z_{ps} in eq 22 to emphasize the fact that this expression defines the value of Z_{exp}. Figure 7 is a plot

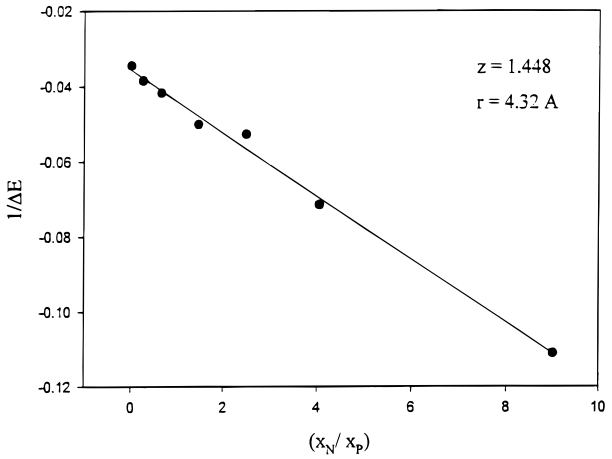

Figure 7. Inverse peak shift (measured against the *n*-hexane peak position) of the ADMA sandwich heteroexcimer (SH) versus ethanol mole fraction. Equation 22 predicts the observed linear dependence. Deviation from linearity occurs when specific interactions contribute to preferential solvation.

of $1/\Delta(\Delta U)$ versus x_n/x_p. Suppan and co-workers have pointed out that specific interactions will cause a sizable deviation from linearity in this plot.[2,3] Thus, the linear result is also consistent with our conclusion that dielectric enrichment is the mechanism of preferential solvation. The slope and intercept in Figure 7 give experimental values of $Z_{exp} = 1.448$ and $a = 4.73$ Å. The value of *a* is within 6% of the value obtained from the slope of Figure 3 and it is within 10% of the van der Waals radius. The parameter Z_{exp} is a composite of preferential solvation and the nonideality of the solvent. The fact that we obtain a linear plot when solvent nonideality is known to exist suggests that Z_{exp} can be decomposed into a sum of contributions from preferential solvation and mixture nonideality,

$$Z_{exp} = Z_{ps} + Z_{ni} \qquad (23)$$

Note that when eq 21 is used to relate ρ_{ps} and Z_{ps}, a linear relationship between these parameters exist for $0 < Z_{ps} < 1.5$. (The linear relationship can be written as $\rho_{ps} = 0.31 \cdot Z_{ps}$, with a correlation coefficient of >0.99) Thus, eq 23 suggests that a similar linear relationship may exist between Z_{exp} and ρ_t, and between Z_{ni} and ρ_{ni}. As a first approximation we use the linear relationship

$$\rho = 0.31 \cdot Z \qquad (24)$$

to calculate Z_{ni} from $\rho_{ni} = 0.22$, and a value of $Z_{ni} = 0.7$ is obtained. If we add Z_{ni} to previously determined independent measures of Z_{ps} given in Table 2, Z_{exp} will range from 1.2 to 1.5, which is in agreement with the value determined from Figure 7.

VII. Discussion

Table 3 gives local mole fractions of the polar component, y_p, of *n*-hexane−ethanol mixtures around the ADMA sandwich heteroexcimer calculated from Z_{ps} using eq 12. The local composition is calculated for each Z_{ps} value given in Table 2, with the exception of Z_{ps} calculated from mean parameter values. Calculations based on the bulk-mole-fraction-weighted (bmfw) radius illustrate the magnitude of dielectric enrichment around ADMA and its dependence on bulk composition. Note, however, that essentially identical values will be found at all bulk compositions by using the value of Z_{ps} determined from mean parameter values. Calculations based on the radii of hexane and

TABLE 3: Local Compositions Around the ADMA Sandwich Heteroexcimer (SH) Dissolved in *n*-Hexane−Ethanol Mixtures[a]

x_p	y_p (Z_{ps} r_{hexane})	y_p (Z_{ps} r_{etoh})	$y_{p,mean}$ (Z_{ps} r_{bmfw})	y_p (from eq 1)
0.100	0.15	0.19	0.15	0.31
0.198	0.28	0.33	0.28	0.47
0.287	0.38	0.44	0.39	0.64
0.401	0.49	0.55	0.51	0.70
0.502	0.59	0.64	0.61	0.76
0.608	0.68	0.72	0.70	0.81
0.801	0.84	0.86	0.86	0.88

[a] Local polar mole fractions (y_p) are calculated from eq 12 using the Z_{ps} values given in Table 2. The Z_{ps} value calculated using the bulk mole fraction weighted (bmfw) radius is presented as the best estimate of the local composition, and the Z_{ps} values calculated using the hexane radius and ethanol radius give extreme values of the local composition. These extreme values are presented to characterize the uncertainty in the estimated local composition. y_p was also calculated using eq 1. Note that eq 1 overestimates the local composition by as much as 100%.

ethanol give estimates of the uncertainty in the calculated compositions. Also included in the table are local compositions calculated using eq 1. Several trends and conclusions can be drawn from these results. First, it is clear that the excess local polar mole fraction (calculated as the ratio of the local increase over the bulk polar mole fraction) is greatest at the lowest bulk polar mole fraction, as is expected on physical grounds. The analysis indicates that the local polar composition can be augmented by >50% at low polar bulk mole fraction. Second, the local composition based on the bmfw radius gives a lower limit to the extent of dielectric enrichment at low bulk polar mole fractions. Note that, though the hexane−ethanol system is important from a practical point of view, it represents a particularly difficult system to analyze on the basis of eq 13, because all of the important solvent parameters that characterize each component have substantially different values. Nevertheless, our analysis in Table 3 indicates that eq 13 can provide a meaningful estimate of the local composition. The third trend that is apparent from Table 3 is that estimates of local composition based on eq 1 grossly overestimate the local polar mole fraction in this system and these estimates exceed even the limiting maximum values by 50%. We surmise that the linear assumption of eq 1 overestimates the local polar mole fraction because it does not properly account for mixture nonideality. Thus, analysis based on eq 1 is likely to attribute mixture nonideality erroneously to specific solvent−solute interaction, which highlights a major limitation of eq 1; that is, it is only valid for ideal dielectric mixtures.

The plot obtained in Figure 4a is linear for neat solvents. This result is not true for all chromophores and fluorophores; in fact, other analogues of ADMA demonstrate a marked deviation from linearity.[21] Mataga has studied the correlation of the LM solvent polarity function with solvatochromic shifts and concludes that a linear plot is obtained when the electronic structure of the probe is not altered by its interaction with the surrounding solvent molecules and the solute excited state is stabilized solely by the electrostatic interaction with the solvent.[18] Generally speaking however, solute−solvent interactions can cause the electronic structure of the probe to change, which would be manifested in a sizable curvature in the energy versus solvent polarity function plot.[21] This fact highlights another caution in the application of eq 1; that is, it is only valid when the spectral property of interest is linear in the solvent polarity function.

Dielectric enrichment is clearly the mechanism of preferential solvation for the ADMA sandwich heteroexcimer dissolved in *n*-hexane−ethanol mixtures. This point is illustrated in Figure 8, where the experimental peak energies are compared with peak energies calculated with eq 14. Equation 14 is modified to include the influence of mixture nonideality by substituting $Z_{total} = Z_{ps} + Z_{ni}$ (see eq 23) in place of Z_{ps}, a parameter that characterizes only preferential solvation. We have used $Z_{ni} = 0.7$, determined experimentally as described in Section VI, and we calculated the peak energies for several bulk compositions. The contribution of dielectric enrichment is characterized at each bulk composition using Z_{ps} values given in Table 2. The Z_{ps} value based on the bmfw radius results in the calculated peak energies, shown in Figure 8, and the Z_{ps} values based on other radii are used to determine the error bars shown in the figure. We obtained excellent agreement between calculated and measured values by this method of analysis. Two conclusions can be drawn from this figure. First, it is clear that specific interactions do not play a role in determining the solvatochromic peak position because such interactions normally cause a red shift of ~30 nm relative to the values calculated from dielectric enrichment equations.[3,15,36] Second, this analysis is based on a postulate that eq 23 can be used to represent the measured peak energies when preferential solvation results only from dielectric enrichment. The success of our analysis based on this postulate suggests that a theoretical basis for eq 23 may be found. We are currently studying this possibility.

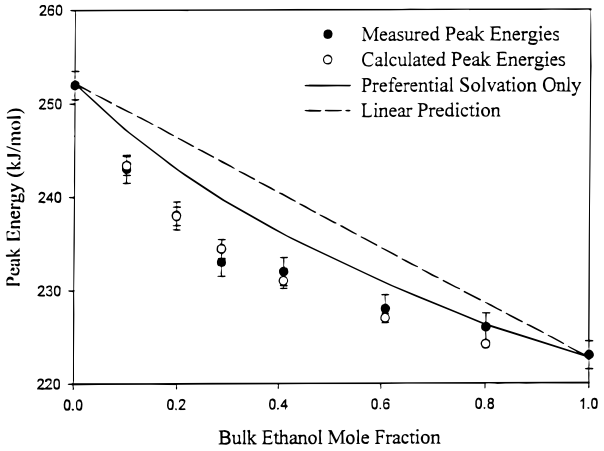

Figure 8. Peak energy of the ADMA sandwich heteroexcimer (SH) versus ethanol mole fraction of the *n*-hexane−ethanol solvent mixture. The filled circles are measured peak energies and the open circles are calculated peak energies. The solid line reflects the contribution of preferental solvation to the peak shift relative to the linear prediction, and the open circles include a contribution from mixture dielectric nonideality. The dashed line is a linear prediction that is expected in the absence of both effects. See Section VII for details of the calculation.

In summary, we have applied Suppan's theory of dielectric enrichment to ADMA dissolved in *n*-hexane−ethanol mixtures. The analysis of the results by several related methods is completely selfconsistent, indicating that dielectric enrichment is the mechanism of preferential solvation in this system. Considering the geometry of the emissive state (folded configuration) and the fact that dimethylaniline is a tertiary amine, the dielectric enrichment mechanism appears to be physically reasonable, and specific interactions do not appear to be at play. We would not necessarily expect this behavior if the solute contained hydrogen-bonding moieties, such as primary amines or alcohols. We are currently designing new studies to examine the influence of specific interactions on solvatochromic peak energies in hydrogen-bonding analogues of ADMA. Based on

our analysis, the solvation shell around ADMA is enriched by >50% over the bulk mixture composition. We have demonstrated that eq 1 is inapplicable to studies in *n*-hexane−ethanol mixtures because it is a nonideal dielectric mixture. We have confirmed previous reports that the sandwich heteroexcimer emission peak of ADMA exhibits a solvatochromic peak energy that is linear in the Lippert−Mataga function. ADMA is more soluble in hexane that ethanol, suggesting that in its ground state, ADMA is nonpolar. Thus, we anticipate that dielectric enrichment is dynamic in this system. These results demonstrate that ADMA is an ideal candidate for studies of dynamics of dielectric enrichment in complex media.

Acknowledgment. We acknowledge Dr. Bob Anderton's role in measuring the dielectric constants of the hexane−ethanol mixtures. We also acknowledge Professor Robert Harris of the University of Missouri Chemistry Department for helpful discussions of Suppan's theory. This research was supported by the National Science Foundation (NSF CHE-9508744) and the University of Missouri Research Board.

References and Notes

(1) Marcus, Y. *Aust. J. Chem.* **1983**, *36*, 1719.
(2) Suppan, P. *J. Chem. Soc., Faraday Trans. 1* **1987**, *83*, 495.
(3) Lerf, C.; Suppan, P. *J. Chem. Soc., Faraday Trans.* **1992**, *88*, 963.
(4) Acree, W. E.; Tucker, S. A.; Wilkins, D. C. *J. Phys. Chem.* **1993**, *97*, 11199.
(5) Acree, W. E.; Tucker, S. A.; Wilkins, D. C. *J. Phys. Chem.* **1994**, *98*, 2537.
(6) Bosch, E.; Roses, M. *J. Chem. Soc., Faraday Trans.* **1992**, *88*, 3541.
(7) Banerjee, D.; Baghchi, S. *J. Photochem. Photobiol. A* **1996**, *101*, 57.
(8) Banerjee, D.; Laha, A. K.; Baghchi, S. *J. Chem. Soc., Faraday Trans.* **1995**, *91*, 631.
(9) Chatterjee, P.; Baghchi, S. *J. Phys. Chem.* **1991**, *95*, 3311.
(10) Szpakowska, M.; Nagy, O. B. *J. Chem. Soc., Faraday Trans. 1* **1989**, *85*, 2891.
(11) Ben-Naim, A. *Cell Biophys.* **1988**, *12*, 255.
(12) Ben-Naim, A. *Statistical Mechanics for Chemists and Biochemists*; Plenum: New York, 1992.
(13) Cichos, F.; Willert, A.; Rempel, U.; Borczyskowski, C. v. *J. Phys. Chem. A* **1997**, *101*, 8179.
(14) Suppan, P. *J. Photochem. Photobiol. A* **1990**, *50*, 293.
(15) Zurawski, W. P.; Scarlata, S. F. *J. Phys. Chem.* **1992**, *96*, 6012.
(16) Petrov, N. K.; Wiessner, A.; Fiebig, T.; Staerk, H. *Chem. Phys. Lett.* **1995**, *241*, 127.
(17) Petrov, N. K.; Wiessner, A.; Staerk, H. *J. Chem. Phys.* **1998**, *108*, 2326.
(18) Mataga, N.; Kubota, T. *Molecular Interactions and Electronic Spectra*; Marcel Dekker: New York, 1970.
(19) (a) Khajehpour, M.; Kauffman, J. F. *Chem. Phys. Lett.* **1998**, *297*, 141; (b) Syage, J. A.; Felker, P. M.; Zewail, A. H. *J. Chem. Phys.* **1984**, 81, 2233.
(20) Liu, C.; Kauffman, J. F. *Rev. Sci. Instrum.* **1996**, *67*, 525.
(21) Masaki, S.; Okada, T.; Mataga, N.; Sakata, Y.; Misumi, S. *Bull. Chem. Soc. Jpn.* **1976**, *44*, 1277.
(22) Chuang, T. J.; Cox, R. J.; Eisenthal, K. B. *J. Am. Chem. Soc.* **1974**, *96*, 6828.
(23) Hui, M.-H.; Ware, W. R. *J. Am. Chem. Soc.* **1976**, *98*, 4718.
(24) Wang, Y.; Crawford, M. C.; Eisenthal, K. B. *J. Am. Chem. Soc.* **1982**, *104*, 5874.
(25) Okada, T.; Migita, M.; Mataga, N.; Sakata, Y.; Misumi, S. *J. Am. Chem. Soc.* **1981**, *103*, 4715.
(26) Migita, M.; Okada, T.; Mataga, N.; Nakashima, N.; Yoshihara, K.; Sakata, Y.; Misumi, S. *Chem. Phys. Lett.* **1980**, *72*, 229.
(27) Migita, M.; Okada, T.; Mataga, N.; Nakashima, N.; Yoshihara, K.; Sakata, Y.; Misumi, S. *Bull. Chem. Soc. Jpn.* **1981**, *54*, 3304.
(28) Crawford, M. K.; Wang, Y.; Eisenthal, K. B. *Chem. Phys. Lett.* **1981**, *79*, 529.
(29) Maroncelli, M.; Kumar, V. P.; Papazyan, A. *J. Phys. Chem.* **1993**, *97*, 13.
(30) Jimenez, R.; Fleming, G. R.; Kumar, P. V.; Maroncelli, M. *Nature* **1994**, *369*, 471.
(31) Reynolds, L.; Gardecki, J. A.; Frankland, S. J. V.; Horng, M. L.; Maroncelli, M. *J. Phys. Chem.* **1996**, *100*, 10337.
(32) Maroncelli, M. *J. Mol. Liq.* **1993**, *57*, 1.
(33) Baumann, W.; Frohling, J.-C.; Brittinger, C.; Okada, T.; Mataga, N. *Ber. Bunsen-Ges. Phys. Chem.* **1988**, *92*, 700.
(34) Bondi, A. *J. Phys. Chem.* **1964**, *68*, 441.
(35) Midwinter, J.; Suppan, P. *Spectrochim. Acta* **1969**, *25A*, 953−958; Ledger, M. B.; Suppan, P. *Spectrochim. Acta* **1967**, *23 A*, 641.
(36) Nitsche, K.-S.; Suppan, P. *Chimia* **1982**, *36*, 346.
(37) Onsager, L. *J. Am. Chem. Soc.* **1936**, *58*, 1486.
(38) Eyring, H.; Jhon, M. S. *Significant Liquid Structures*; John Wiley & Sons: New York, 1969.
(39) Orge, B.; Iglesias, M.; Rodriguez, A.; Canosa, J. M.; Tojo, J. *Fluid Phase Equil.* **1997**, *133*, 213.
(40) Ormanoudis, C.; Dakos, C.; Panaylotou, C. *J. Chem. Eng. Data* **1991**, *36*, 39.
(41) Dean, J. A. *Lange's Handbook of Chemistry*; McGraw-Hill: New York, 1992.